IPPP/05/12
DCPT/05/24
13th April 2005

Diffractive $W + 2$ jet production: a background to exclusive $H \to WW$ production at hadron colliders

V.A. Khoze[a,b], M.G. Ryskin[a,b] and W.J. Stirling[a,c]

[a] Department of Physics and Institute for Particle Physics Phenomenology, University of Durham, DH1 3LE, UK

[b] Petersburg Nuclear Physics Institute, Gatchina, St. Petersburg, 188300, Russia

[c] Department of Mathematical Sciences, University of Durham, DH1 3LE, UK

Abstract

Central exclusive double diffractive Higgs boson production, $pp \to p \oplus H \oplus p$, is now recognised as an important search scenario for the LHC. We consider the case when the Higgs boson decays to two W bosons, one of which may be off-mass-shell, that subsequently decay to the $q\bar{q}l\nu$ final state. An important background to this is from the QCD process $gg \to Wq\bar{q}$, where the two gluons are required to be in a $J_z = 0$, colour-singlet state. We perform an explicit calculation and investigate the salient properties of this potentially important background process.

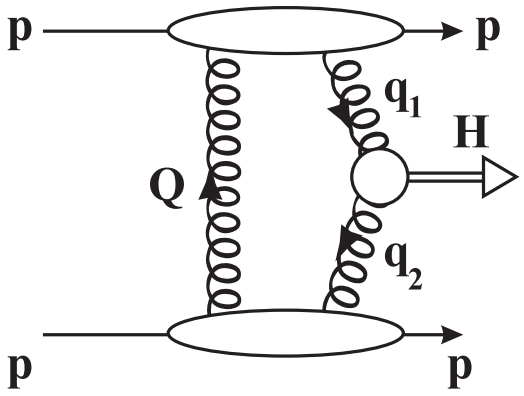

Figure 1: Schematic diagram for central exclusive Higgs production at the LHC, $pp \to p+H+p$.

1 Introduction

Within the last few years the unique environment for investigating new physics using forward proton tagging at the LHC has become fully appreciated, see for example [1, 2, 3, 4, 5, 6] and references therein. Of particular interest is the 'central exclusive' Higgs boson production $pp \to p \oplus H \oplus p$. The $\oplus$ signs are used to denote the presence of large rapidity gaps; here we will simply describe such processes as 'exclusive', with 'double-diffractive' production being implied. In these exclusive processes there is no hadronic activity between the outgoing protons and the decay products of the central system. The predictions for exclusive production are obtained by calculating the diagram of Fig. 1 using perturbative QCD [7, 1]. In addition, we have to calculate and include the probability that the rapidity gaps are not populated by secondary hadrons from the underlying event [8] .

There are three reasons why central exclusive production is so attractive. First, if the outgoing protons remain intact and scatter through small angles then, to a very good approximation, the primary active di-gluon system obeys a $J_z = 0$, CP-even selection rule [9, 10]. Here J_z is the projection of the total angular momentum along the proton beam axis. This selection rule readily permits a clean determination of the quantum numbers of the observed Higgs-like resonance which will be dominantly produced in a scalar state. Secondly, because the process is exclusive, the energy loss of the outgoing protons is directly related to the mass of the central system, allowing a potentially excellent mass resolution, irrespective of the decay mode of the produced particle.[1] And, thirdly, a signal-to-background ratio of order 1 (or even better) is achievable, even with a moderate luminosity of 30 fb^{-1} [2, 4]. In some MSSM Higgs scenarios central exclusive production provides an opportunity for lineshape analysing [3, 5] and offers a way for direct observation of a CP-violating signal in the Higgs sector [12, 5]. The analysis in [7, 2, 3] was focused primarily on light SM and MSSM Higgs production, with the Higgs decaying to 2 $b-$jets. The potentially copious $b-$jet (QCD) background is controlled by a combination of the spin-parity selection rules [9, 10], which strongly suppress leading-order

[1] Recent studies suggest that the missing mass resolution σ will be of order 1% for a 140 GeV central system, assuming both protons are detected at 420m from the interaction point [11, 4].

$b\bar{b}$ production, and the mass resolution from the forward proton detectors. The missing mass resolution is especially critical in controlling the background, since poor resolution would allow more background events into the mass window around the resonance. Assuming a mass window $\Delta M \sim 3\sigma \sim 3-4$ GeV, it is estimated that 11 signal events, with a signal-to-background ratio of order 1, can be achieved with a luminosity of 30 fb^{-1} in the $b\bar{b}$ decay channel [10, 2].[2] Whilst the $b\bar{b}$ channel is theoretically very attractive, allowing direct access to the dominant decay mode of the light Higgs boson, there are some basic problems which render it challenging from an experimental perspective, see [13] for more details. First, it relies heavily on the quality of the mass resolution from the proton taggers to suppress the background. Secondly, triggering on the relatively low-mass dijet signature of the $H \to b\bar{b}$ events is a challenge for the Level 1 triggers of both ATLAS and CMS. And, thirdly, this measurement requires double $b-$tagging, with a corresponding price to pay for tagging efficiencies. In Ref. [13], attention was turned to the WW^* decay mode of the light Higgs Boson, and above the 2 W threshold, the WW decay mode.[3] This channel does not suffer from any of the above problems: suppression of the dominant backgrounds does not rely so strongly on the mass resolution of the detectors, and, certainly, in the semi-leptonic decay channel of the WW system Level 1 triggering is not a problem. The advantages of forward proton tagging are, however, still explicit. Even for the double leptonic decay channel (i.e. with two leptons and two final state neutrinos), the mass resolution will be very good, and of course observation of the Higgs in the double tagged channel immediately establishes its quantum numbers. It is worth mentioning that the mass resolution should improve with increasing Higgs mass [11]. Moreover, the semileptonic 'trigger cocktail' may allow the combination of signals not only from $H \to WW$ decays but also from the $\tau\tau$, ZZ and even the semileptonic $b-$decay channels.

The central exclusive production cross section for the Standard Model Higgs boson was calculated in [7, 1]. In Fig. 2 we show the cross section for the process $pp \to pHp \to pWWp$ as a function of the Higgs mass M_H at the LHC. The increasing branching ratio to $WW^{(*)}$ (from 12% at $M_H = 120$ GeV to $\sim 100\%$ at 160 GeV) as M_H increases (see for example [14]) compensates for the falling central exclusive production cross section. For comparison, we also show the cross section times branching ratio for $pp \to pHp \to pb\bar{b}p$. Here, and in what follows, we use version 3.0 of the HDECAY code [15]. For reference purposes, the cross sections in Fig. 2 are normalised in such a way that $\sigma_H = 3$ fb for $M_H = 120$ GeV.

Note also that nowadays there is renewed interest in MSSM scenarios with low $\tan\beta$. This is because the most recent value of the top quark mass weakens the low $\tan\beta$ exclusion bounds from LEP (see for example [16]), and the experimental coverage of this range of the MSSM parameter space becomes more attractive. In Fig. 2 we show the results for $\tan\beta = 2, 3, 4$. Evidently the expected central exclusive diffractive production yield is promising in the low $\tan\beta$ region.

[2] It is worth noting that certain regions of MSSM parameter space can be especially 'proton tagging friendly'. For example, at large $\tan\beta$ the situation becomes exceptionally favourable, with predicted Higgs signal-to-background ratios in excess of 20 [3]. In this particular case the tagged proton mode may well be *the* discovery channel.

[3] Note that the rate of detectable events from $H \to ZZ$ decay is very low — less than 10% of the $H \to WW$ rate — and we shall not consider this channel further here.

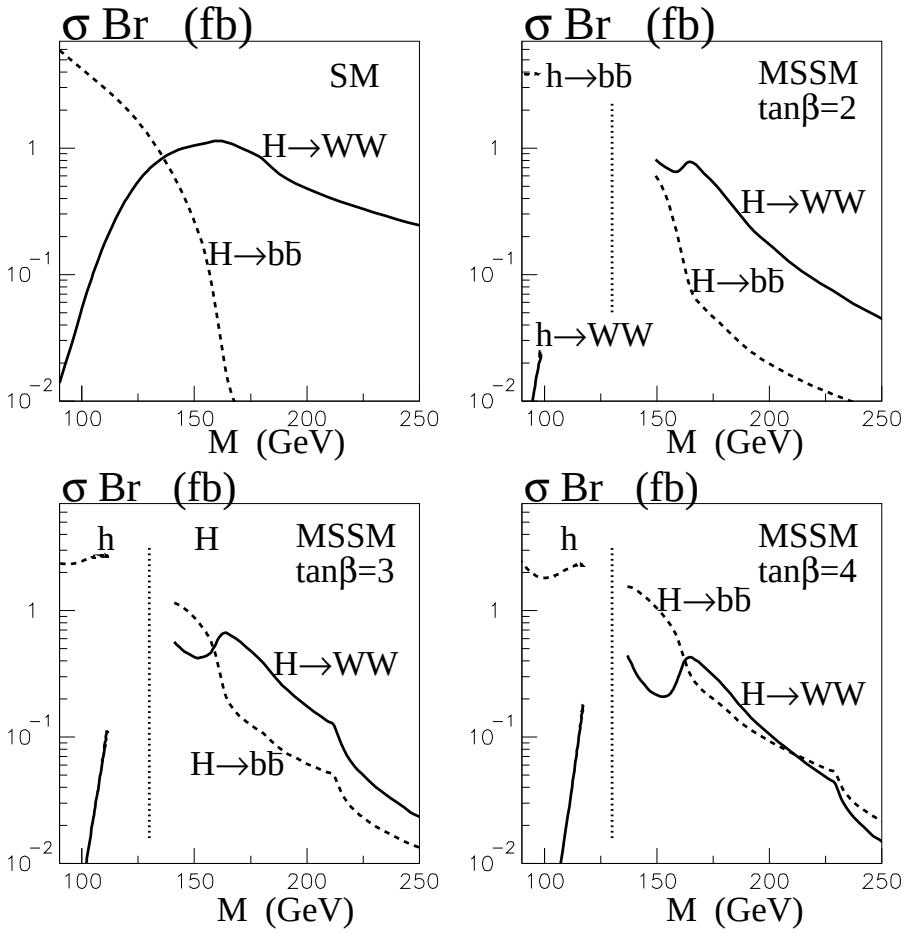

Figure 2: The cross section times branching ratio for the central exclusive production of the MSSM Higgs boson (with three values of $\tan\beta = 2, 3, 4$) as a function of Higgs mass in the WW and $b\bar{b}$ decay channels. The cross section for Standard Model Higgs boson production is also shown.

Experimentally, events with two W bosons in the final state fall into 3 broad categories — fully-hadronic, semi-leptonic and fully-leptonic — depending on the decay modes of the W's. Events in which at least one of the Ws decays in either the electron or muon channel are by far the simplest, and Ref. [13] focuses mainly on these semi- and fully-leptonic modes. As mentioned above, one of the attractive features of the WW channel is the absence of a relatively large irreducible background, *cf.* the large central exclusive $b\bar{b}$ QCD background in the case of $H \to b\bar{b}$, suppression of which relies strongly on the experimental missing mass resolution and di-jet identification.

The primary exclusive backgrounds in the case of the WW channel can be divided into two broad categories:

1. Central production of a WW^* pair $pp \to p + (WW^*) + p$ from either the (a) $\gamma\gamma \to WW^*$ or (b) $gg^{PP} \to WW^*$ subprocess.

2. The W-strahlung process $pp \to p + Wjj + p$ originating in the $gg^{PP} \to Wq\bar{q}$ subprocess, where the W^* is 'faked' by the two quarks.

Here the notation gg^{PP} indicates that each active gluon comes from a colour-singlet $t-$channel (Pomeron) exchange and that the di-gluon state obeys the $J_z = 0$, parity-even selection rule. As shown in [13], over a wide region of Higgs masses the photon-photon backgrounds are strongly suppressed if we require that the final leptons and jets are central and impose cuts on the transverse momenta of the protons in the taggers. Using the results of Ref. [17], we find that the QCD quark-box-diagram contribution from the $gg^{PP} \to WW^*$ subprocess is also very small, on the level of 1% of the signal yield. The most important background therefore comes from the second category above, i.e. from the W-strahlung process exemplified by the diagrams of Fig. 3. Here we have to take into account the $J_z = 0$ projection of this amplitude, which requires a calculation of the individual helicity amplitudes. This can be done, for example, using the spinor technique of Ref. [18]. The primary aim of this paper is to investigate the salient properties of this potentially important background process.

2 The $gg \to Wq\bar{q}$ $J_z = 0$ colour-singlet hard process

The tree-level $\mathcal{O}(\alpha_S^2 \alpha_W)$ process $gg \to Wq\bar{q}$ is one of many processes that contribute to $W+2$ jet production at hadron colliders, and as such it has been studied intensively as part of the 'QCD' background to W^+W^-, $t\bar{t}$ etc. production. The scattering amplitude was first calculated almost twenty years ago in Ref. [18], using the new (at that time) spinor techniques that were developed for multiparton tree-level scattering amplitudes. Nowadays, all the spin- and colour-summed amplitudes contributing to inclusive $W + 2$ jet production are easily obtained from automated tree-level matrix element software packages such as MADGRAPH [19].

However in the present context we are specifically interested in the $J_z = 0$, colour-singlet projection of the $gg \to Wq\bar{q}$ process. It is difficult to extract such projections from the standard packages, and so we have performed the calculation from first principles using the original techniques of Ref. [18].

It is interesting to compare the structure of the inclusive and projected amplitudes. For the former, there are a total of 8 Feynman diagrams, two involving the triple-gluon vertex ($gg \to g^* \to Wq\bar{q}$) and six diagrams corresponding to the six different permutations of the three gauge bosons attached to the quark line. Two of the latter are shown in Fig. 3. Three of the six diagrams correspond to an interchange of the two gluons, and so the sum and difference of these amplitude triplets (labelled A_{123} and A_{456}) contribute to even and odd colour factors respectively. Schematically, then, we have for the inclusive case:

$$\begin{aligned}
|\mathcal{M}|^2(J_z=0) &= \frac{28}{3}\left(|A_{123}(++)+A_{456}(++)|^2+|A_{123}(--)+A_{456}(--)|^2\right) \\
&+ 12\left(|A_{123}(++)-A_{456}(++)+2A_{78}|^2+|A_{123}(--)-A_{456}(--)+2A_{78}|^2\right) \\
|\mathcal{M}|^2(J_z=2) &= \frac{28}{3}\left(|A_{123}(+-)+A_{456}(+-)|^2+|A_{123}(-+)+A_{456}(-+)|^2\right) \\
&+ 12\left(|A_{123}(+-)-A_{456}(+-)|^2+|A_{123}(-+)-A_{456}(-+)|^2\right) \qquad (1)
\end{aligned}$$

where the labels $(++)$ etc. are the helicities of the incoming gluons (the quark helicities being fixed once the sign of the W boson is specified), and the even and odd colour factors are

$$\begin{aligned}
\frac{28}{3} &= \mathrm{Tr}[(T^aT^b+T^bT^a)(T^aT^b+T^bT^a)] \\
12 &= \mathrm{Tr}[(T^aT^b-T^bT^a)(T^bT^a-T^aT^b)] \qquad (2)
\end{aligned}$$

Note that the diagram with the $s-$channel gluon contributes only to the colour-odd, $J_z=0$ amplitude. In the fully inclusive $W+2$ jet calculation, the two spin contributions of Eq. (1) are of course added together.

For the background to exclusive $H \to WW$ production, Fig. 1, we need the $J_z=0$, colour-singlet projection:

$$|\mathcal{M}|^2(J_z=0, \text{colour singlet}) = \frac{64}{3}\left(|A_{123}(++)+A_{456}(++)+A_{123}(--)+A_{456}(--)|^2\right) \qquad (3)$$

where now the colour factor is

$$\frac{64}{3} = 4\ \mathrm{Tr}[T^aT^aT^bT^b] \qquad (4)$$

The colour-octet $s-$channel gluon diagrams (A_{78}) no longer contribute to the $J_z=0$ amplitude. Note also that the $(++)$ and $(--)$ spin components can interfere in the overall amplitude squared. This is because in the case of exclusive central diffractive production, the amplitudes (rather than the cross sections) should be averaged over the helicities $(++)$ or $(--)$ of the incoming gluons, see for example [1].

In the following section we present some numerical results based on the above calculations.

3 Numerical results and discussion

The $gg^{PP} \to Wq\bar{q}$ cross section is obtained by integrating the matrix element squared of the previous section over an appropriate region of three-body phase space. However care must be taken in avoiding collinear singularities. These occur when either one or both of the incoming

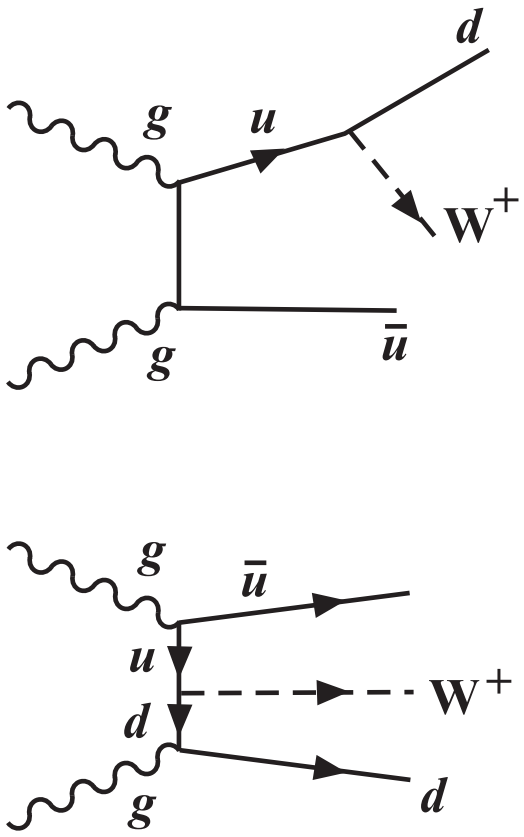

Figure 3: Examples of Feynman diagrams contributing to the $J_z = 0$, colour-singlet $gg \to Wq\bar{q}$ process.

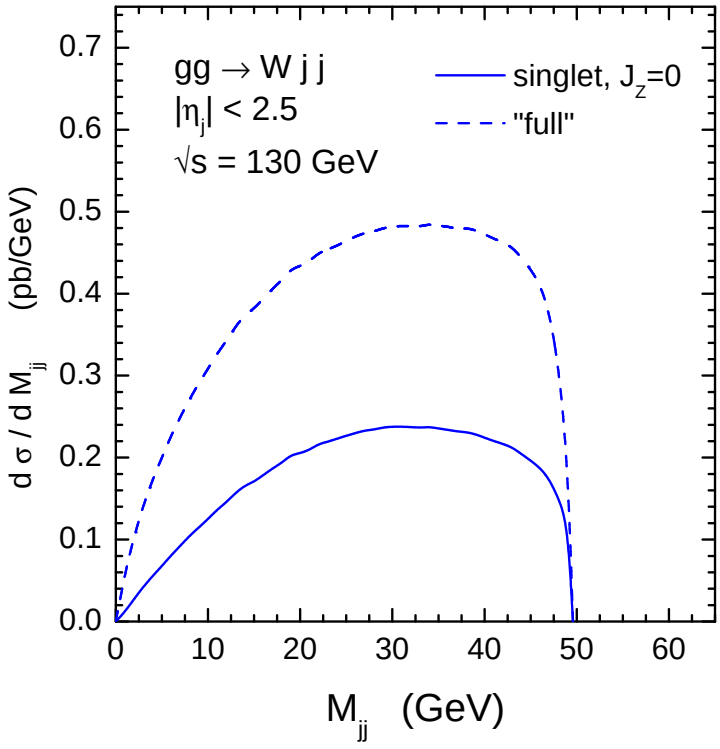

Figure 4: The $J_z = 0$, colour-singlet $gg \to Wq\bar{q}$ cross section of Eq. (3) compared to the spin- and colour-summed cross section of Eq. (1). The gg centre-of-mass energy is $\sqrt{s} = 130$ GeV, and the final-state quark jets are required to lie in the pseudorapidity range $-2.5 < \eta_j < +2.5$.

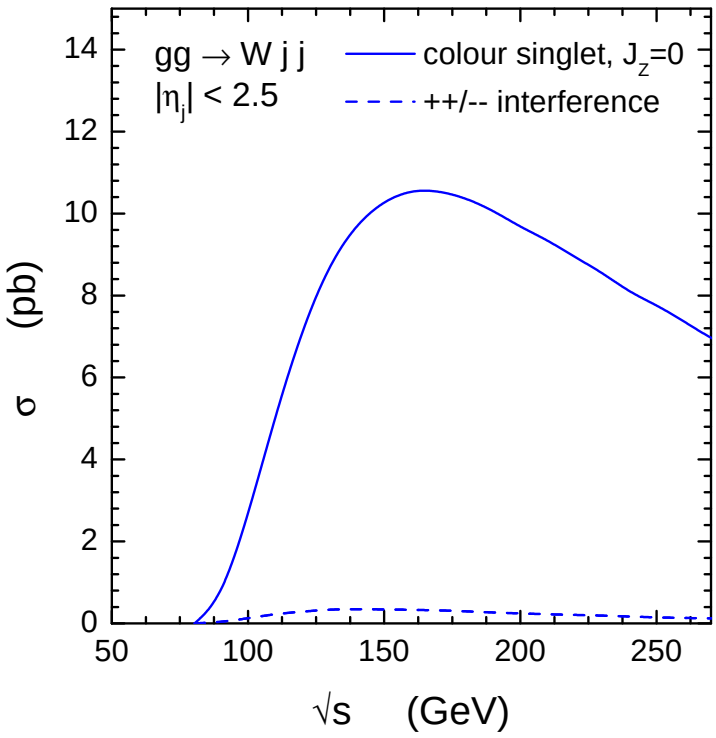

Figure 5: The scattering energy dependence of the $J_z = 0$, colour-singlet $gg \to Wq\bar{q}$ cross section of Eq. (3). The final-state quark jets are required to lie in the pseudorapidity range $-2.5 < \eta_j < +2.5$. Also shown (dashed line) is the contribution of the interference between the $(++)$ and $(--)$ gluon helicity amplitudes in Eq. (3).

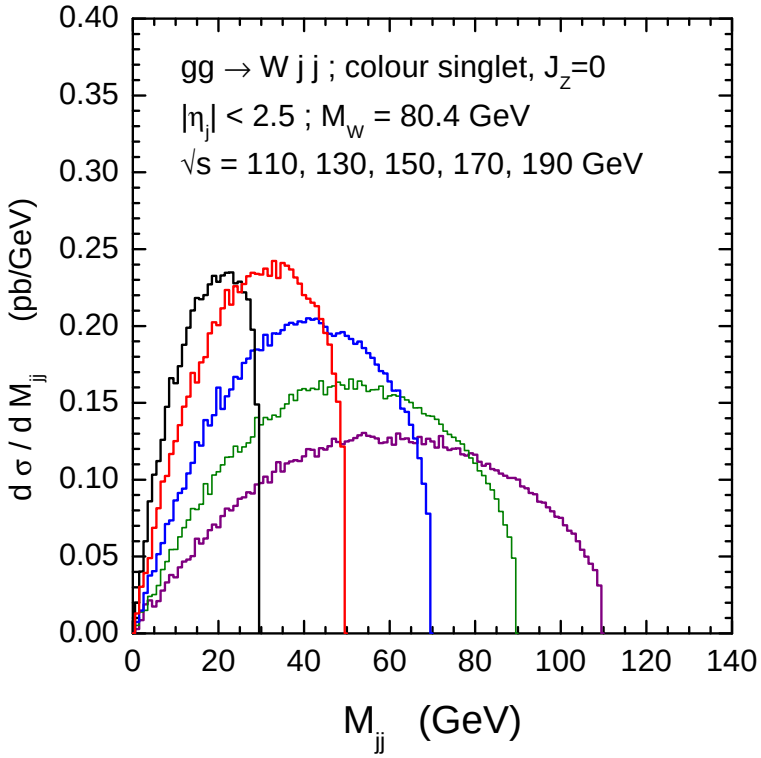

Figure 6: The jet-jet ($q\bar{q}$) invariant mass distribution for $J_z = 0$, colour-singlet $gg \to Wq\bar{q}$ production for different values of the gg centre-of-mass energy $\sqrt{s}$. The final-state quark jets are required to lie in the pseudorapidity range $-2.5 < \eta_j < +2.5$. The end point for each distribution is at $M_{jj} \approx \sqrt{s} - M_W$.

gluons splits into a collinear $q\bar{q}$ pair. Of course in this case the final-state (zero transverse momentum) quarks would not be registered as jets in the detector. In order to have observable jets and to suppress the collinear logarithmic singularities, we impose the pseudorapidity cut ($|\eta_j| < 2.5$) on the final-state quarks. With these minimal cuts, we obtain a finite background cross section with which to compare the Higgs signal.

Figure 4 shows the jet-jet mass distribution $d\sigma/dM_{jj}$ for the inclusive and $J_z = 0$, colour-singlet projected $gg \to Wq\bar{q}$ process at $\sqrt{s} = 130$ GeV, a typical value for the Higgs mass. Two families of fermions are summed over in the final state (i.e. the quarks are either u, d, s or c) and both $W^+q\bar{q}$ and $W^-q\bar{q}$ configurations are included. Evidently the $J_z = 0$, colour-singlet projection suppresses the cross section by about a factor of 2 for these kinematics. In Fig. 5 we show the total $gg^{PP} \to Wq\bar{q}$ cross section as a function of the gluon-gluon centre-of-mass energy $\sqrt{s}$. The dashed line is the contribution of the interference between the $(++)$ and $(--)$ gluon helicity amplitudes in Eq. (3). This is evidently a very small effect for these kinematics. Finally, Fig. 6 shows the jet-jet ($q\bar{q}$) invariant mass distribution for different values of $\sqrt{s}$.

From Fig. 5 we see that the $gg \to Wq\bar{q}$ total cross section is about 7.2 (9.8) pb for $\sqrt{s} =$ 120 (140) GeV, rising to 10.6 pb at $\sqrt{s} \simeq 160$ GeV and then decreasing slowly for higher energies. When comparing to the Higgs $\to WW^{(*)}$ or WW signal, this background cross section should be multiplied by the phase space factor $2\Delta M/M_H$, where $\Delta M \sim 3\sigma$ is the mass window over which we collect the signal, and by the corresponding gluon luminosity at $\sqrt{s_{gg}} = M_H$ [1]. Assuming that $2\Delta M/M_H \sim 0.1$ we finally arrive at the background cross section at $\sqrt{s} = 14$ TeV of about 1.7 fb for $M_H = 140$ GeV. This is a 'maximal' background cross section in the sense that the only cuts on the final-state jets — apart from the mass-window requirement — are the weak rapidity cuts $|\eta_j| < 2.5$ imposed in the jet-jet centre of mass system. Further laboratory-frame cuts on jet and lepton rapidity and transverse momentum will further reduce the background cross section, but will of course also reduce the signal, though to a lesser extent. Comparing with Fig. 2, we see that the $Wq\bar{q}$ background cross section is about a factor of two larger than the Standard Model Higgs signal[4] at this value of M_H.

It might appear that the QCD background could be further reduced by only selecting the subset of events with a rather large two-jet mass M_{qq}, in order to mimic the $W^{(*)} \to q\bar{q}$ signal. However as shown in Fig. 7, when $M_H < 2M_W$ and one of the W bosons is off-mass-shell, the M_{W^*} distribution is peaked *below* the edge of phase space at $M_{W^*} \simeq M_H - M_W$. The reason for this (see, for example, Ref. [20]) is that below the nominal WW threshold the three-body phase space factor compensates the variation of the W Breit-Wigner distribution in the tail. Indeed, the M_{W^*} distribution actually vanishes at $M_{W^*} = M_H - M_W$ (where here M_H denotes the c.m.s. energy of the WW^* system). On the other hand, for a low mass $M_{W^*} < M_W$ the variation of the Breit-Wigner factor is controlled mainly by the difference $M_W - M_{W^*} > \Gamma_{W,\mathrm{tot}}$. Because of this, the M_{W^*} mass distribution becomes quite wide, and the peak is shifted below the edge of phase space by an amount of order $2M_W - M_H$. Comparing the signal and background jet-jet invariant mass distributions, Figs. 7 and 6, we see that while the S/B ratio could be improved slightly by imposing a minimum M_{jj}, the loss of signal events would not lead to any overall

[4]Strictly, in this comparison the signal cross sections in Fig. 2 should be reduced slightly to take into account the $W \to \sum q\bar{q}$ branching ratio and the rapidity acceptance of the jets.

improvement in the statistical significance of the signal. Note that we have not investigated further optimisation procedures, such as the cuts on the final-state lepton angles and azimuthal correlations between the quark jets, which may further improve the signal-to-background ratio.

It is obvious from Figs. 6 and 7 that above the WW threshold the situation becomes more favourable, since the background contribution can now be reduced by requiring the invariant mass of the di-quark system to be close to M_W. Moreover, at higher Higgs masses the mass resolution of the proton taggers is expected to improve [11].

Returning to the case when $M_H < 2M_W$, we have so far concentrated on the case when it is the *off-shell* W^* that decays hadronically, the on-shell W decaying leptonically. There will of course be an equal number of signal events when this situation is reversed and the W^* decays leptonically.[5] Therefore apart from around the threshold region $\sqrt{s} \sim 2M_W$, the M_{jj} distribution for the full $q\bar{q}l\nu$ sample of the signal will have a double-peak structure, corresponding to the superposition of a Breit-Wigner distribution peaked around $M_{jj} \sim M_W$ with a broader distribution peaked at lower mass, see Fig. 7. The QCD W-strahlung process calculated above is only a background to the former component of the signal.[6] The only other potentially significant background contributions for the $M_{jj} \sim M_W$ case come from the photon-photon fusion $\gamma\gamma \to WW^*$ subprocess and from the gluon-gluon fusion $gg^{PP} \to WW^*$ subprocess mediated by a quark loop. As discussed in Ref. [13], the former ($\gamma\gamma$) contribution can be strongly (about 10 times) reduced by imposing cuts on the forward proton transverse momenta, $p_t > 100 - 200$ MeV/c. Using the results of [17], we estimate that the QCD quark box-diagram $gg^{PP} \to WW^*$ contribution is very small, on the level of 1% of the signal yield. Therefore, the statistical significance for these type of events is very high: for events with $p_t > 100$ MeV/c the expected signal-to-background ratio S/B is of the order of 10. This makes the channel with the leptonic W^*-decay especially attractive when $M_H < 2M_W$. We expect that a detailed Monte Carlo simulation of both signal and background events of this type would lead to a set of signal-enhancing experimental cuts, reflecting the specific kinematics of these processes.

In summary, we have considered in detail the exclusive production and decay to WW or W^* of a Higgs boson in conjunction with two forward protons at the LHC. We have focused on the $q\bar{q}l\nu$ final state, which constitutes just less than half the signal. For $M_H < 2M_W$, there are two distinct scenarios in which either the W or the W^* decays leptonically. For the former, we identified and calculated the QCD background, showing it to be of similar magnitude to the (Standard Model) Higgs boson signal. We expect that the situation could be improved somewhat by optimising the cuts on the final-state particles. In the second scenario in which the W^* decays leptonically, the background is expected to be very small. Overall, then this process offers a promising way of detecting the Higgs boson, either in the Standard Model or in particular supersymmetric extensions.

[5] The ratio of fully hadronic, mixed hadronic-leptonic and fully leptonic decay channels for $H \to WW^*$ is rough $4:4:1$, with the mixed channel split evenly between the case when the W or the W^* decays leptonically.

[6] Actually, there will still be a QCD background contribution from $W^*q\bar{q}$ production with $W^* \to l\nu$ and $M_{q\bar{q}} \sim M_W$, but this will be very small.

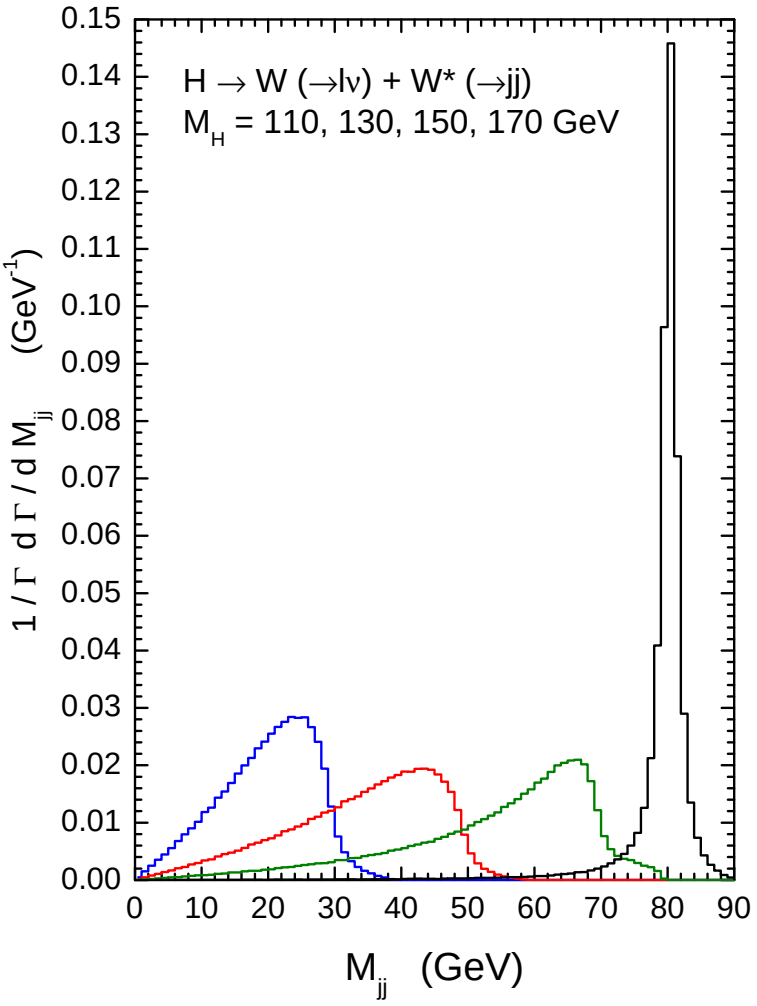

Figure 7: The jet-jet ($q\bar{q}$) invariant mass distribution for the signal process $H \to W(\to l\nu) + W^*(\to q\bar{q})$, for different values of the Higgs boson mass. For $M_H > 2M_W$, the jet-jet mass distribution assumes a Breit-Wigner form. The distribution integrates to 0.5 in each case.

Acknowledgements

We thank Mike Albrow, Brian Cox, Albert De Roeck, John Ellis, Jeff Forshaw, Alan Martin, Sasha Nikitenko, Risto Orava, Krzystof Piotrzkowski and Georg Weiglein for useful discussions. MGR thanks the IPPP at the University of Durham for hospitality. This work was supported by the UK Particle Physics and Astronomy Research Council, by a Royal Society special project grant with the FSU, by grant RFBR 04-02-16073 and by the Federal Program of the Russian Ministry of Industry, Science and Technology SS-1124.2003.2.

References

[1] V.A. Khoze, A.D. Martin and M.G. Ryskin, Eur. Phys. J. **C23** (2002) 311.

[2] A. De Roeck, V.A. Khoze, A.D. Martin, R. Orava and M.G. Ryskin, Eur. Phys. J. **C25** (2002) 391.

[3] A.B. Kaidalov, V.A. Khoze, A.D. Martin and M.G. Ryskin, Eur. Phys. J. **C33** (2004) 261.

[4] B. Cox, `arXiv:hep-ph/0409144`.

[5] J. Ellis, Jae Sik Lee and A. Pilaftsis, `arXiv:hep-ph/0502251`.

[6] M. Boonekamp, R. Peschanski and C. Royon, Phys. Lett. **B598** (2004) 243;
V.A. Petrov, R.A. Ryutin, A.E. Sobol and J.-P. Guillaud, `arXiv:hep-ph/0409118`.

[7] V.A. Khoze, A.D. Martin and M.G. Ryskin, Eur. Phys. J. **C14** (2000) 525.

[8] V.A. Khoze, A.D. Martin and M.G. Ryskin, Eur. Phys. J. **C18** (2000) 167.

[9] V.A. Khoze, A.D. Martin and M.G. Ryskin, `hep-ph/0006005`, in *Proc. of 8th Int. Workshop on Deep Inelastic Scattering and QCD (DIS2000)*, Liverpool, eds. J. Gracey and T. Greenshaw (World Scientific, 2001), p.592.

[10] V.A. Khoze, A.D. Martin and M.G. Ryskin, Eur. Phys. J. **C19** (2001) 477, erratum **C20** (2001) 599.

[11] R. Orava, talk presented at the Workshop *"The Future of Forward Physics at the LHC"*, Manchester, 12–14 December 2004.

[12] V.A. Khoze, A.D. Martin and M.G. Ryskin, Eur. Phys. J. **C34** (2004) 327.

[13] B. Cox *et al.*, in preparation.

[14] M. Carena and H. Haber, Prog. Part. Nucl. Phys. **50** (2003) 63;
G. Degrassi, S. Heinemeyer, W. Hollik, P. Slavich and G. Weiglein, Eur. Phys. J. **C28** (2003) 133.

[15] A. Djouadi, J. Kalinowski and M. Spira, Comput. Phys. Com. **108** (1998) 56, arXiv:hep-ph/9704448.

[16] LHWG–Note 2004-01, http://lephiggs.web.cern.ch/LEPHIGGS/papers/index.html; S. Heinemeyer, W. Hollik and G. Weiglein arXiv:hep-ph/0412214, and references therein.

[17] M. Duhrssen, K. Jakobs, P. Marquard and J.J. van der Bij, arXiv:hep-ph/0504006.

[18] R. Kleiss and W.J. Stirling, Nucl. Phys. **B262** (1985) 235.

[19] T. Stelzer and W.F. Long, Phys. Commun. **81** (1994) 357.

[20] T. Sjöstrand and V.A. Khoze, Z. Phys. **C62** (1994) 281.